

## Scour and erosion experience with flexible debris-flow nets

Nadine Feiger<sup>a,\*</sup>, Corinna Wendeler<sup>b</sup>

<sup>a</sup>*Department of Civil, Environmental and Geomatic Engineering ETH Zurich, Stefano-Franscini-Platz 5, Zürich 8093, Switzerland*

<sup>b</sup>*Geobrugg AG, Achstrasse 11, Romanshorn 8590, Switzerland*

---

### Abstract

Flexible debris-flow nets were developed in the frame of a three-year PhD thesis by Wendeler in 2008. Since then, they have been used all over the world for debris-flow protection or slope/riverbed stabilization. Some of these installed flexible debris-flow nets have already been filled a couple of times and verified the developed load model. Nevertheless, depending on soil properties, most problems with debris-flow nets appear to be related to construction, such as channel flank erosion, which exposes anchors, or undermines supporting foundations. Both cases lead to instability of the entire system and to increased maintenance costs and should therefore be avoided. In this contribution, we present a service ability method for scour and erosion issues on flexible debris-flow nets. In this context, “service ability method” means a design tool that should help to suggest construction possibilities to avoid erosion problems along the barrier in order to guarantee a lifetime of more than 25 years. The results are based on an analysis of existing barriers to determine occurring scour and erosion problems. Hence, an approach to calculate scour and erosion length and depth respectively around the barrier construction is developed. To validate this approach, a debris-flow simulation with the software RAMMS, or equivalent software, is used. In terms of economic efficiency, different construction measures for riverbed and flank stabilization are analyzed and implemented into the service ability. This tool will help designers and planning engineers to design and calculate their debris-flow protection system in a more economic and safe way. Further, maintenance costs will be minimized and a longer lifetime of the entire barrier system, including the anchors as the most cost-intensive parts, can be provided. Since the project is still ongoing, the final design tool with its equations cannot yet be discussed in detail in the following paper.

"Keywords: Flexible ring net, Debris flow, Service ability"

---

### 1. Introduction

Floods, debris flows, and slope failures are the most common natural hazards in Switzerland. In inhabited areas, material and personal damages occur from time to time. Therefore, investigations about debris-flow dynamics and protective structures have been a research topic for many years (e.g. Böll, 1997; Bergmeister, 2009). To increase knowledge about debris-flow behavior, several small- to large-scale flume experiments were recently conducted (e.g. Weber, 2003; de Haas et al., 2015; Major, 1997) and described (e.g. Iverson, 1997; Kowalski, 2008) worldwide. Nowadays, various mitigation structures are available against natural hazards, but erosion around them is a notable problem.

One possible mitigation structure against debris flows is flexible ring nets. Until 2005, flexible nets were mainly used for rockfall barriers. Retained slides in these nets were observed, but there was no existing dimensioning concept which proved that these nets are capable of retaining large slides. As a result, real-scale experiments with flexible ring nets were performed at Illgraben test site in Switzerland between 2005 and 2008 (Wendeler, 2008). At least once per year a middle ( $10'000 - 20'000\text{m}^3$ ) to large ( $> 50'000\text{m}^3$ ) debris flow naturally occurs in the Illgraben and is suitable to test and improve flexible ring nets. Tests showed that a single barrier can retain debris-flow material until its retaining capacity is reached, depending on the channel geometry. Afterwards the material can overflow the barrier without damaging the system. Therefore, a so-called multi-level system, with several barriers in a row, can be planned and constructed. Such a multi-level system was tested at Hasliberg and Merdenson (Switzerland) (Wendeler et al., 2008).

---

\* Corresponding author e-mail address: [nadine\\_feiger@hotmail.com](mailto:nadine_feiger@hotmail.com)

Based on these tests, a dimensioning concept was developed by Wendeler (2008) and led with load distribution and simulation with the finite-element software FARO (Volkwein, 2004) to standardized flexible ring net barriers. Since then, flexible ring net barriers have been installed worldwide. Some of them have already been filled a couple of times. Experiences over the past ten years showed that most problems with ring nets appear to be related to construction, such as channel flank erosion, which exposes anchors or undermines supporting foundations.

We present an initial progress on developing a service ability method based on an analysis of existing barriers, 1:1 field test, an intermediate-scale flume experiment and a debris flow simulation with Rapid Mass Movement Simulation (RAMMS) (WSL Institute for Snow and Avalanche Research SLF) to help designers and planning engineers to design and calculate their debris flow protection systems in a more economic and safe way. Furthermore, the lifetime of these flexible net systems can be optimized by protecting them against erosion and scour processes.

## **2. Study site and data**

To develop an appropriate service ability method, scour and erosion problems on existing flexible ring nets have been analyzed. The main database provides 80 installed flexible ring net barriers in Switzerland since 2005 by Geobruigg AG. Few debris-flow events occurred in Switzerland since then, and therefore, data from filled barriers in Italy, Spain and Peru were additionally used. All installed flexible ring nets in Switzerland will be found on Geobruigg's web page with information about installation year, barrier type, occurred events and problems beginning in May 2019.

Calculation of possible erosion scenarios are based on commonly used equations in river and hydraulic engineering. Developed erosion scenarios are validated by new erosion data collected in an intermediate-scale flume experiment in 2018/2019. Within the same data set, behavior of a slope stabilization mesh (TECCO®) as erosion protection was tested. In addition, 1:1 field data with slope stabilization meshes are collected at Illgraben, Switzerland from December 2018 until June 2019. Experimental small-scale data from (Speerli, 2009), large-scale data from (Bugnion et al., 2012) and observations at Illgraben by WSL were used for comparison. Further data were required to simulate and verify the developed service ability with the Rapid Mass Movement Simulation (RAMMS) debris-flow module. These included (a) a digital elevation model (DEM), (b) a hydrograph or (c) a release area.

## **3. Methods**

To develop a service ability concept, major problems have to be identified and their corresponding solutions designed. First, erosion in a mountain torrent can be triggered by a debris-flow event or normal water flow, for example due to rain. The design should cover both cases. Second, important parameters such as channel geometry, barrier type, soil properties and soil mechanical properties must be detected. Hence, possible scour areas related to flexible ring net barriers were identified upstream and downstream of a barrier construction (Fig. 1). In practice, a barrier overflow can lead to erosion and scours downstream of the barrier (Fig. 1c), whereas a construction post behaves as a pile scour and can lead to undermining of the foundation (Fig. 1d). In case of the barrier filling process or depending on the flow depth, flank erosion occurs at the anchors (Fig. 1a).

To quantify these erosion and scours, different calculation formulas can be found in the literature. However, none of them are directly suitable for mountain torrents. To verify an appropriate approach, 1:1 field test (Section 3.1) and an intermediate-scale flume experiment was conducted (Section 3.2). Comparison with experimental data by Speerli (2009), Bugnion (2012), natural Illgraben events and RAMMS simulation led to the final design.

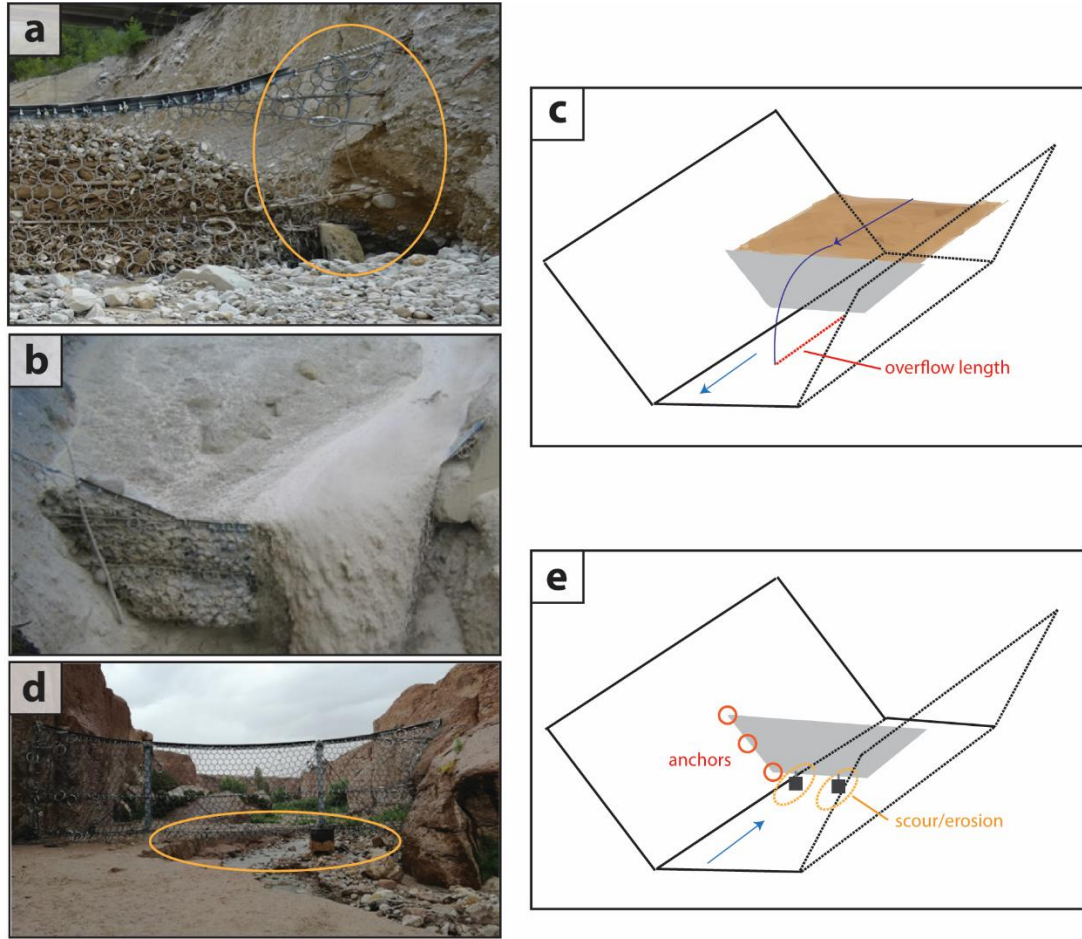


Fig. 1. Examples of erosion/scour problems on flexible ring net and schematic overview. (a) Eroded anchors; (b) Filled barrier with an overflow; (c) schematic overview of erosion problem in case of an overflow; (d) undermined foundations due to riverbed erosion; (e) Schematic overview upstream erosion problem of the barrier (anchors due to flank erosion, and foundation due to riverbed erosion).

### 3.1. 1:1 field installation

In rivers, riprap or concrete bolts are commonly used for erosion protection; however, a slope stabilization mesh with or without a geotextile layer is another possible option. There are no data or experiences of such a mesh in a mountain torrent. To evaluate the effectiveness of stabilization mesh on erosion control, a Geobrugg AG slope stabilization mesh was installed at Illgraben (Switzerland) from December 2018 until June 2019 (Fig. 2). Two different mesh types G65/3 and G45/2 were chosen and installed. One only the mesh and one with the corresponding geotextile. In total, four meshes with a 3.9 m width were anchored with ramming nails (Fig. 2a and 2b). Based on the torrent topography, it was not possible to install the mesh in the middle of the torrent bed as well as to cover the mesh edges by a rope (Fig. 2a and 2b). In general, the mesh is anchored by a raster system and on all edges by a top, bottom and lateral boundary rope to fix the mesh as tightly as possible onto the slope (Fig. 2c).

Erosion and mesh behavior were observed by a time series of pictures, which were mostly taken after rain events. After a significant event, estimation of acting shear force ( $\tau$ ) was carried out by a RAMMS simulation and calculation according to Equation 1:

$$\tau = \rho \cdot g \cdot h \cdot J \quad (1)$$

where  $\rho$  = density,  $g$  = gravitational acceleration,  $h$  = flow depth, and  $J$  = channel inclination.

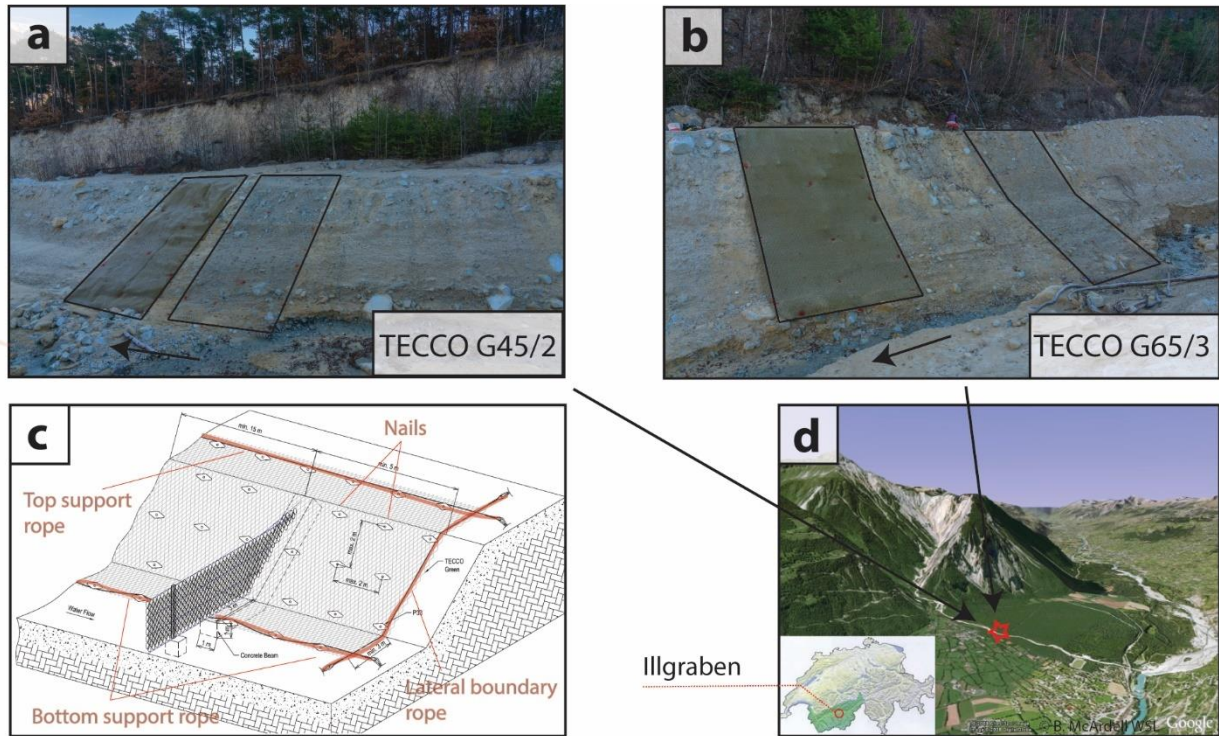


Fig. 2. (a) TECCO G45/2 with TECMAT (brown) and without (grey); (b) TECCO G65/3 with TECMAT (brown) and without (grey), Arrow indicates flow direction; (c) Schematic TECCO erosion protection (d) Study site overview.

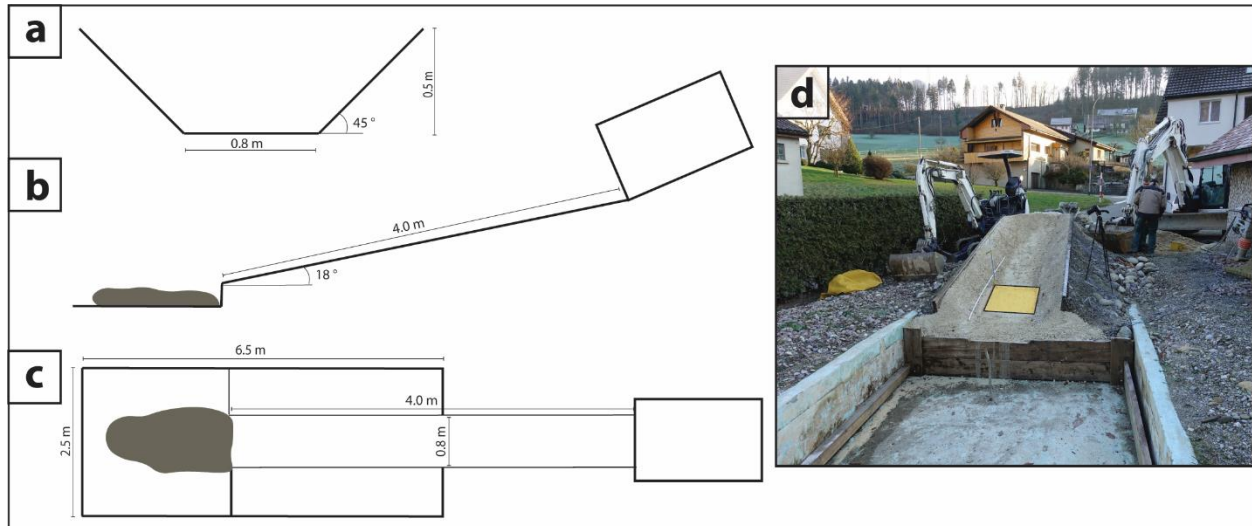


Fig. 3. Schematic flume experiment view. (a) Channel cross section; (b) Side view; (c) Plan view; (d) Flume with force plate (yellow).

### 3.2. Flume experiment

To obtain data on overflow length - distance from the net to the impact of the discharge jet - (Fig. 1c), shear force, and erosion behavior of a slope stabilization mesh, an intermediate-scale flume was constructed as shown in Fig. 3. Flume geometry was determined by the available space and to be on a scale of around 1:10 to 1:15 (Fig. 3a-c). No laser sensors were available, therefore, flow velocity ( $u$ ) and flow depth ( $h$ ) were estimated by a high-speed camera. Shear ( $\tau$ ) and pressure force ( $N$ ) were measured with a force plate (Fig. 3d), which was already used by Bugnion

(2012). The shear and force plates were calibrated and sampled at a rate of 1 kHz. One flume flank is covered with the slope stabilization mesh (G45/2). The used slope material was taken from the Illgraben. The original Illgraben material was used for the debris-flow mud mixture. The release of smaller mud mixture amount (0.05-0.2 m<sup>3</sup>) was done by an excavator shovel, and larger amounts by a concrete mixer.

In the first experiment series, different material volumes were released to identify the relation between measured shear force and Froude numbers ( $Fr$ ). During that, erosion underneath the slope stabilization mesh was observed with images. In a second experiment series, overflow length of flows past a ring net barrier that was installed in the flume 2.5 meters downstream of the release point were evaluated. In these experiments, a single debris-flow release filled the net. Additional flows were released and the length of overflow past the net was measured.

Collected shear force data were transformed from  $kg$  into  $kN/m^2$  and for each experiment its Froude number ( $Fr$ ) was calculated according to Equation 2:

$$Fr = \frac{u}{\sqrt{g \frac{A}{b}}} \quad (2)$$

where  $u$  = flow velocity,  $g$  = gravitational acceleration,  $A$  = cross-sectional area, and  $b$  = water level width.

To be able to compare our measured shear forces with the measurements made at different scales by Bugnion (2012) and measured at Illgraben (McArdell, 2016), the shear stress is converted to be a dimensionless number alpha ( $\alpha$ ) as shown in Equation 3:

$$\alpha = \frac{\frac{\tau_{characteristic}}{\mu}}{\frac{\tau_{measured}}{\mu}} = \frac{\frac{u}{h}}{\frac{\tau_{measured}}{\mu}} \quad (3)$$

where  $\tau_{char}$  = characteristic shear force defined as  $u/h$  = flow velocity over flow depth (shear rate),  $\tau_{measured}$  = measured shear force, and  $\mu$  = viscosity.

Overflow length (Fig. 1c) calculation was done according to Equations 4-6 for each overflow event, as well as for existing data from Speerli (2009) and video recorded Illgraben events. Calculated lengths were then compared with the measured ones in the experiment. The most fulfilling equations were used for the design tool to determine the overflow length.

Equation 4 is used for dimensioning stilling basin length (Bergmeister, 2009):

$$L_T = (u + \sqrt{2 \cdot g \cdot h}) \cdot \sqrt{\frac{H}{g}} + h \quad (4)$$

where  $L_T$  = stilling basin length,  $u$  = flow velocity,  $g$  = gravitational acceleration,  $h$  = flow depth, and  $H$  = construction height.

Equation 5 determines the overflow length based on the trajectory parabola with inclination:

$$L_P = (H + h) \cdot \tan(\alpha) + u \sqrt{\frac{2(H+h)}{g \cdot \cos(\alpha)}} \quad (5)$$

where  $L_P$  = trajectory length,  $\alpha$  = slope inclination,  $g$  = gravitational acceleration,  $h$  = flow depth, and  $H$  = construction height.

Equation 6 is used to calculate hydraulic jump length for inclined channels (Jirka et al., 2009):

$$L_w = (6.1 + 4.0 J) \cdot h_2 \quad (6)$$

where  $L_w$  = hydraulic jump length,  $J$  = channel inclination,  $h_2$  = flow depth downstream the barrier and  $h_2 = \frac{h_1}{2} (\sqrt{1 + 8 Fr^2} - 1)$  with  $h_1$  = flow depth upstream the barrier, and  $Fr$  = Froude number.

Further, other equations can be found in literature such as from Smetana, Rouse, and others (Bollich, 2013) that are used for stilling basin length dimensioning. All of them are based on an empirical number and the  $h_2$  term. Therefore, an empirical number was determined for the taken flume experiment data to improve the equation.



### 3.3. Service ability design

The service ability design works as a decision-making tool (Fig. 4). First, parameters, such as channel geometry, barrier type, soil properties and soil mechanical properties are added. Based on this input information and the most suitable equation identified in Section 3.2, a recommendation according to erosion can be made. Based on that a possible mitigation system (slope stabilization mesh, concrete bolts, riprap or a combination of them) can be suggested to ensure a long lifetime of the barrier.

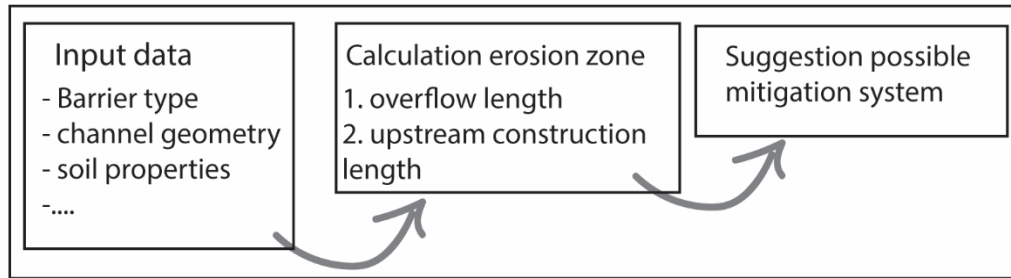


Fig. 4. Schematic overview of service ability tool.

## 4. Results and Discussion

Since the project is still ongoing, some first results will be presented here. Note that they are not completed yet.

### 4.1. Field observation

Two weeks after slope stabilization mesh installation (3 December 2018) either a debris flow or flood event with significant sediment transport occurred at Illgraben. Unfortunately, all installed observation measurement devices (geophones, laser sensor etc.) from WSL (Swiss Federal Institute for Forest, Snow and Landscape Research) were not operating in December 2018. Figure 5 shows the slope stabilization meshes after the event. Flow depth is clearly visible, as well as erosion on the upstream and downstream side of the mesh. Upstream side mesh erosion could be expected due to the lack of a lateral boundary rope and the fact that the mesh is not as tight to the slope as it normally is when it gets anchored. However, ramming nails were not displaced by the event.

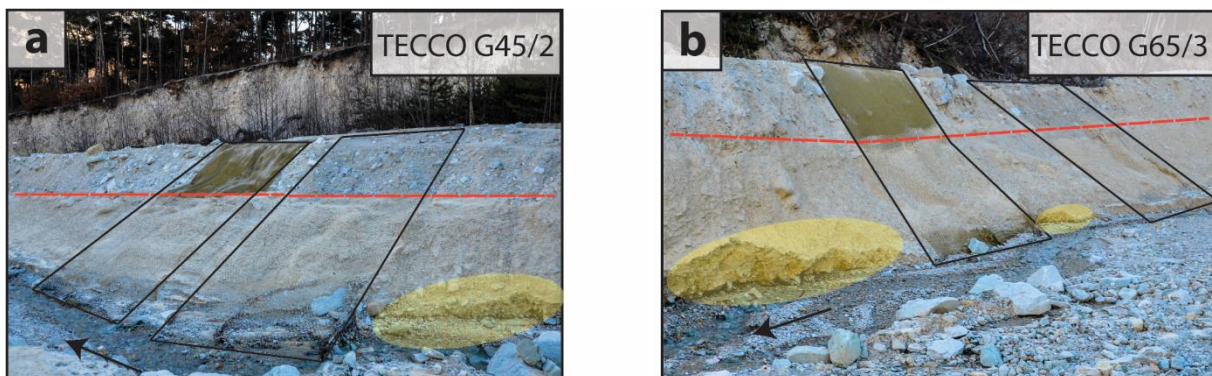


Fig. 5. Installed slope stabilization mesh (rectangular) after debris flow event of 3 December 2018. Red dashed line shows flow depth, yellow ellipse indicates erosion up- and downstream the mesh. Flow direction is indicated by the arrow.

Table 1 shows calculated shear force for the event on 3 December 2018 based on Equation 1, for granular flow as well as mud flow at two Illgraben locations. One at the mesh location with  $J=0.05$ ,  $h=3$  m and the other at the measurement device location with  $J=0.09$ ,  $h=1.5$  m. Comparison with 2006 recorded data, one can assume that the event was approximately the size of  $10'000-18'000\text{m}^3$ . A comparison with a RAMMS simulation is ongoing.

Table 1. Shear force results at Illgraben.

	Shear force ( $kN/m^2$ ) mesh location	Shear force ( $kN/m^2$ ) measurement device location
Granular flow ( $\rho=2150 \text{ kg/m}^3$ )	3.2	2.8
Mud flow ( $\rho=1900 \text{ kg/m}^3$ )	2.8	2.5

#### 4.2. Flume experiment

Reliable overflow length determination based on actual overflow events at Illgraben is almost impossible. Some overflow events are larger than the recorded video section. Therefore, one can only approximately say the overflow is larger than ten meters or smaller than ten meters. However, a first overflow length estimation based on recorded videos from Speerli (2009) experiments can be done as well as from our first flume experiments. Besides, overflow length according to Equation 4-6 can be calculated for this data as well as for Smetana. Percentage deviation for each trial from the calculated value (trajectory parabola with inclination, stilling basin, hydraulic jump, and Smetana) are shown in Figure 6. Trial 1-5 are data form Speerli (2009) and 6-15 from realized flume experiments.

As expected, the length results for the stilling basin (orange dots) underestimate the measured results due to the lack of a slope correction factor within the equation. The trajectory parabola (blue dots) fluctuates around the measured values and has the lowest deviation from measured lengths. The expectation was that the hydraulic jump (green dots) would deviate most. The equation according to Smetana ( $L_S = 3 \cdot (\sqrt{1 + 8Fr_1^2} - 3)$ ) (yellow dots) is basically the hydraulic jump with additional empirical values and one can see that it already deviates less. However, all of these equations have their limitations and are designed for water. Since all of them depend on the flow depth, flow velocity and hence, the Froude number, a sensitivity analysis was conducted (not shown in this paper). So far one can state that the flow depth uncertainty with respect to measurement error does not account as much as the velocity for the deviation from the measured value. To identify the optimal domain to use the equation, the results for each equation will be correlated with the Froude number. Consequently, the equations to use for the service ability tool will result out of that analysis. These results will be presented at the presentation.

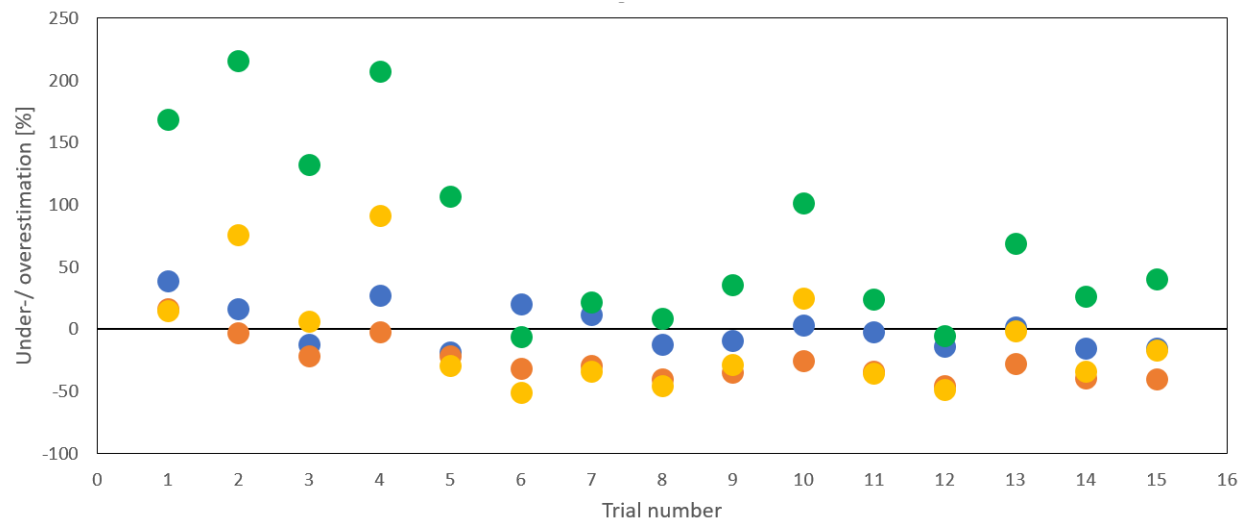


Fig. 6. Percentage deviation from measured Trial (zero line) to calculated trajectory parabola with inclination (blue), stilling basin (orange), hydraulic jump (green), and Smetana (yellow).

Some first results of dimensionless numbers ( $\alpha$ ) and Froude number ( $Fr$ ) were calculated from available Illgraben data. The regression indicates a quadratic behavior, but a final statement cannot be made, since the results from the flume experiments are not fully analyzed.

## 5. Conclusion and Outlook

So far, no finalized conclusion can be made. The 1:1 field installation is under observation and during the winter months no significant event is expected. RAMMS simulation of the observed event is running. Flume experiments to determine overflow length are completed and shear force experiments are ongoing. Afterwards, interpretation of the data will allow the determination of equations to describe a lower and upper bound for the construction length. Measured shear forces will be analyzed and compared with the measured Illgraben data. Finally, the service ability design can be programmed and tested. The tool will be presented at the presentation.

The eventual creation of the tool describes an overall start for guidelines and help to design a sustainable flexible ring net barrier. Further tests, experiments and especially experience are necessary to improve service ability on flexible ring net barriers.

## Acknowledgements

This project was done within a master thesis frame at the Swiss Federal Institute of Technology in Zurich, Switzerland (ETHZ) in collaboration with Geobrug AG, Switzerland. A grateful acknowledgement to Geobrug AG for the opportunity to realize such a project and for all the assistance and helpful discussions. Especially, A. Lanter, S. Karrer and R. Wyss for helping in the field. Thanks to B. McArdell for sharing Illgraben knowledge and data from Swiss Federal Institute for Forest, Snow and Landscape Research (WSL).

## References

- Bergmeister, K., 2009, *Schutzbauwerke gegen Wildbachgefahren: Grundlagen, Entwurf und Bemessung, Beispiele*: John Wiley and Sons, 121 p.
- Bollrich, G., 2013, *Technische Hydromechanik 1: Grundlagen*, Berlin: Beuth Verlag GmbH, 289.
- Böll, A., 1997, *Wildbach- und Hangverbau: Berichte der Eidgenössischen Forschungsanstalt für Wald, Schnee und Landschaft*, Nr. 343.
- Bugnion, L., McArdell, B. W., Bartelt, P., and Wendeler, C., 2012, Measurements of hillslope debris flow impact pressure on obstacles: *Landslides*, v 9(2), p. 179-187, doi: 10.1007/s10346-011-0294-4.
- Haas, T., Braat, L., Leuven, J. R., Lokhorst, I. R., and Kleinhans, M. G., 2015, Effects of debris flow composition on runout, depositional mechanisms, and deposit morphology in laboratory experiments. *Journal of Geophysical Research: Earth Surface*, p. 1949-1972, doi: 10.1002/2015JF003525.
- Iverson, R. M., 1997, The physics of debris flows. *Reviews of geophysics*, p. 245-296.
- Jirka, G. H., and Lang, C., 2009, *Einführung in die Gerinnehydraulik*. Karlsruhe: Universitätsverlag Karlsruhe, 69 p.
- Kowalski, J., 2008, *Two-phase modeling of debris flows* [Ph.D. thesis]: Zurich, ETH Zurich.
- Major, J. J., 1997, Depositional Processes in Large-Scale Debris-Flow Experiments: *The Journal of Geology*, p. 345-366, doi: 10.1086/515930.
- McArdell, B. W., 2016, Field Measurements of Forces in Debris Flows at the Illgraben: Implications for Channel-Bed Erosion: *International Journal of Erosion Control Engineering*, p. 194-198, doi: 10.13101/ijece.9.194.
- Speerli, J., 2009, *Murgang Modellierung*. Rapperswil: Institut für Bau und Umwelt (unpublished).
- Volkwein, A., 2004, *Flexible Murgangbarrieren: Bemessung und Verwendung*. Birmensdorf: Berichte der Eidgenössischen Forschungsanstalt für Wald, Schnee und Landschaft, v. 8.
- Weber, D., 2003, *Untersuchungen zum Fliess- und Erosionsverhalten granularer Murgänge* [Ph.D. thesis]: Zurich, ETH Zurich.
- Wendeler, C. S., 2008, *Murgangrückhalt in Wildbächen: Grundlagen zu Planung und Berechnung von flexiblen Barrieren* [Ph.D. thesis]: Zurich, ETH Zurich.
- Wendeler, C., Volkwein, A., Roth, A., Herzog, B., Hahlen, N., and Wenger, M., 2008, Hazard prevention using flexible multi-level debris flow barrier, on *Proceedings, Interpraevent, 11th, Dornbirn: Voralberg, Austria*, p. 547-554.